

# Beam Angular Divergence Effects in Ion Implantation

T.N. Horsky<sup>1</sup>, M. I. Current<sup>2</sup>, S. K. Hahto<sup>1</sup>, D. G. Bilbrough<sup>1</sup>, D. C. Jacobson<sup>1</sup>,  
W. A. Krull<sup>1</sup>, R. D. Goldberg<sup>1</sup>, N. Hamamoto<sup>3</sup>, and S. Umisedo<sup>3</sup>

<sup>1</sup>*SemEquip Inc., 34 Sullivan Road, Suite 18, Billerica, MA 01862, USA*

<sup>2</sup>*Current Scientific, 1729 Comstock Way, San Jose, CA, 95124 USA*

<sup>3</sup>*Nissin Ion Equipment Co., 575 Kuze Tonoshiro-cho, Minami-ku, Kyoto, Japan, 601-8205*  
*e-mail: thorsky@semequip.com*

**Abstract.** An important difference between monomer ion beams and heavy molecular beams is a significant reduction in beam angular divergence and increased on-wafer angular accuracy for molecular beams. This advantage in beam quality stems from a reduction in space-charge effects within the beam. Such improved angular accuracy has been shown to have a significant impact on the quality and yield of transistor devices [1,12]. In this study,  $B_{18}H_x^+$  beam current and angular divergence data collected on a hybrid scanned beam line that magnetically scans the beam across the wafer is presented. Angular divergence is kept below 0.5 deg from an effective boron energy of 200 eV to 3000 eV. Under these conditions, the beam current is shown analytically to be limited by space charge below about 1 keV, but by the matching of the beam emittance to the acceptance of the beam line above 1 keV. In addition, results of a beam transport model which includes variable space charge compensation are presented, in which a drift mode  $B_{18}H_x^+$  beam is compared to an otherwise identical boron beam after deceleration. Deceleration is shown to introduce significant space-charge blow up resulting in a large on-wafer angular divergence. The divergence effects introduced by wafer charging are also discussed.

**Keywords:** molecular implantation, ion beam, angular divergence

**PACS:** 61.72Tt

## INTRODUCTION

The need for near-“diffusion-less” anneal conditions to achieve  $\approx 10$  nm junction depths for CMOS source/drain extensions has placed stringent requirements on the implantation process for the vertical and lateral placement of dopant and other ions in close matching to the needs of the transistor design. Considerable effort and ingenuity has been incorporated in the design of ion beam lines and wafer scanning systems to provide consistent control of beam incidence angle over the wafer surface to within a small fraction of a degree [1]. Next, control of the optical properties of the ion beam itself, including the beam divergence, is an increasingly relevant issue.

The impact of highly divergent ion beams, such as those created by accel-decel optics, on local dopant uniformity near gate and mask edges has been noted since the early days of sub-keV high current implanters [2]. These dopant uniformity effects included under-dosing due to beam shadowing and local over-dosing due to ion scattering from gate and mask edges. Indications of additional effects due to local disruptions of space charge balances by device-scale structures were seen in the current-voltage characteristics for 0.5 keV  $B^+$  beams implanted into sub-micron mask openings [3].

The recent introduction of heavy molecular ion beams has demonstrated several advantages for high dose, low energy doping of semiconductors, including higher throughput for  $p^+$  doping, enabling of defect-free junctions with reduced junction leakage, improved

activation and contact resistance, as well as providing self-amorphizing implants for simplified and lower cost process flows [4,5,6]. The additional advantages of decreased beam divergence for molecular ion beams has been noted in the increased control of threshold voltage distributions and improved drive current symmetry for 40 nm CMOS transistors [7].

## Space Charge Limits on Beam Transport

The space charge-limited charge density at ion extraction, the so-called Child-Langmuir relation, can be expressed as:

$$J_{max} = 1.72 (Q/m)^{1/2} V^{3/2} d^{-2}, \quad (1)$$

Where  $J_{max}$  is in mA/cm<sup>2</sup>,  $Q$  is the ion charge state,  $m$  is the ion mass in AMU,  $V$  is the extraction voltage in kV, and  $d$  is the gap width in cm. While derived for a planar diode, this relation is also applicable to beam transport, particularly for an uncompensated beam. In practice, beam ionization of residual gases provides some charge compensation through low-energy electron capture by the beam potential, although the ionization cross sections fall steeply below about 10 keV. Plasma floods also provide useful compensation, although they tend to provide their primary benefit at their point of use, their thermal electrons being localized by fields present in the beam line. Wafer charging is a continuing yield concern for advanced devices, and is typically controlled by the incorporation of a plasma flood near the wafer surface.

The cluster implant process requires only one electrical charge per cluster of  $n$  atoms, rather than requiring every dopant atom to carry one electrical charge, largely ameliorating wafer charging for large  $n$ . The transport efficiency (beam transmission) can also be improved by using ionized clusters, since the dispersive Coulomb force is reduced with a reduction in charge density. Implanting a cluster of  $n$  like atoms provides the equivalent of a much lower energy monatomic implant since each atom of the cluster is implanted with the ion energy divided by  $n$ , whereas the implanter is also operated at an extraction voltage about  $n$  times higher than the required monomer implant energy.

By extension of equation (1), the following figure of merit,  $\Delta$ , can be defined to quantify the increase in throughput, or implanted dose rate, for a cluster ion implant relative to monomer implantation:

$$\Delta = n (U_n / U_1)^{3/2} (m_n / m_1)^{-1/2}. \quad (2)$$

Here,  $\Delta$  is the maximum relative improvement in dose rate (atoms/sec) achieved by implanting a cluster with  $n$  atoms of the dopant of interest at an energy  $U_n$  relative to the single atom implant of an atom of mass  $m_1$  at energy  $U_1$ , where  $U_i = eV_i$ . In the case where  $U_n$  is adjusted to give the same dopant implantation depth as the monatomic ( $n=1$ ) case, equation (2) reduces to:

$$\Delta = n^2. \quad (3)$$

Thus, the implantation of a cluster of  $n$  dopant atoms has the potential to provide a dose rate  $n^2$  higher than the conventional implant of single atoms.

## EXPERIMENTAL METHOD AND DATA

Ion beam characteristics were measured on a magnetically scanned implanter whose design has been previously disclosed [8]. As shown in Figure 1, the system consists of ClusterIon<sup>®</sup> source, 120° analyzer magnet, quadrupole triplet, scanner, and collimator. Beam diagnostics located behind the wafer plane to measure spatial uniformity, size, parallelism, and current, have also been described previously [9].

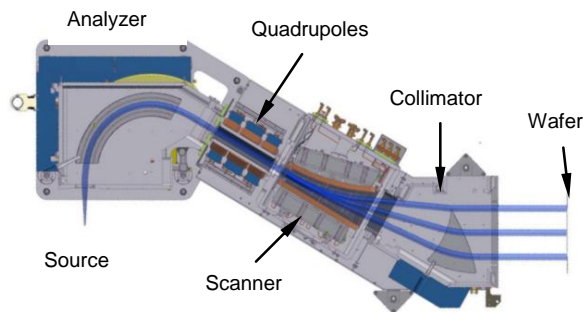


**FIGURE 1.** Beam line test system. Diagnostics are directly behind the wafer position.

Beam angle measurements were carried out with multiple Faraday cup systems (front & back Faraday arrays) located about 300 mm upstream and downstream of the wafer. The beam parallelism (beam incident angle across the wafer) was calculated by comparing the relationship of the beam position vs. time between the front and back Faraday arrays. In addition, as the beam profile can be measured at each Faraday, the nominal beam divergence  $\alpha_p$  was determined by comparing the average beam diameter at FWHM between these Faraday arrays.

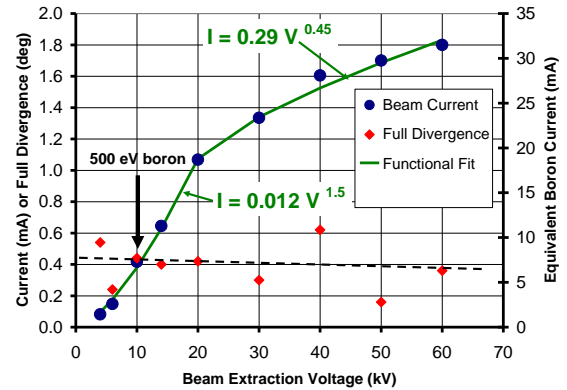


**FIGURE 2.** On-wafer currents and full divergence angles for scanned  $B_{18}H_x^+$  beams as a function of energy.

Figure 2 shows scanned  $B_{18}H_x^+$  beam current (circles) and full divergence angle (diamonds) as measured by the system of Figure 1. The divergence data and related dashed trend line show that beam divergence remained relatively constant over the energy range 4 keV to 60 keV, centered about 0.4 degrees. We define the full beam divergence  $\phi$  as:

$$\phi = 2 |\alpha_p| \quad (4)$$

Where  $\alpha_p$  is the half-pencil angle about the beam axis. Since divergence is small throughout the energy range (corresponding to an equivalent boron implant range of 200eV to 3keV), the principal effect of energy on beam transport is an increase in beam current with increasing energy. We have therefore fitted the beam current data of Figure 2 with the following binary function:

$$I = 0.012 V^{1.5}, \quad 4 \text{ kV} \leq V \leq 20 \text{ kV}; \quad (5)$$

$$I = 0.29 V^{0.45}, \quad 20 \text{ kV} < V \leq 60 \text{ kV}. \quad (6)$$

This function suggests that in the low energy regime (below about 1 keV effective boron energy), transport is limited principally by space charge, as expressed by Eq. (1), whereas at higher energies, transmission is limited principally by the acceptance of the beam line. The fundamental premise underlying latter conclusion

can be seen by examining the 2D beam emittance,  $\epsilon_{2D}$ , according to Eq. (7):

$$\epsilon_{2D} = (\pi/2) D (v_T/v_{||}), \quad (7)$$

Where  $D$  is the beam diameter, and  $v_T$  and  $v_{||}$  are the ion velocities transverse to and along the beam direction, respectively, in the dispersive plane. Since  $(v_T/v_{||})$  is clearly proportional to  $V^{1/2}$ , we conclude that transmission at higher energies is principally determined by matching of the beam emittance to the acceptance of the beam line.

## Beam Transport Modeling

To better understand the effects of space charge on the average angle the beam makes with the wafer, we modeled two ion beams, the first carrying 7.5 mA of boron at 500 eV, the second carrying 0.42 mA of  $B_{18}H_x^+$  beam at 10 keV. In practice, these beams would deliver the same dose rate and implant energy to the wafer, the first presumably after deceleration, and the second in drift. We assumed the same source emittance and beam divergence after mass analysis and before deceleration, about 0.5 m before the wafer.

Lorentz 2D V6.4 from Integrated Engineering Software, Inc. was used to generate the model. Rays were launched from identical initial positions to create a Gaussian current density. This density was scaled according to the particular ion current being launched. The ions were launched from a surface to create a divergent beam, and then accelerated over a very short gap to the final required energy before allowing the ion to drift for 0.5 m and impact on the wafer. Space charge was calculated and stored in a mesh as described in the Lorentz 2D V6.4 user's manual [10]. Output generated included trajectory directional vectors that were used to determine the beam angle and pencil angle at the wafer.

The divergence of the decelerated boron beam will be a function of three terms: the emittance of the beam, lens aberrations introduced by the decel stage, and space-charge blowup of the decelerated beam. Lens aberrations were not included in this model. The divergence increase of the decelerated boron beam due to a fixed beam emittance was derived from equations (4) and (7), *i.e.*,  $\phi_{boron} \sim (10kV/0.5kV)^{1/2} \phi_{B18} \approx 4.5$  times the  $B_{18}H_x^+$  divergence, or about 1.9 deg. Figure 3 shows the output for a 10 keV, 0.42 mA  $B_{18}H_x^+$  beam with 43% space charge compensation. The divergence at the wafer predicted by the model for these conditions is 2 degrees. Figure 4 shows the output for a 500 eV, 7.5 mA  $^{11}B^+$  beam with 98% space charge compensation. The model predicts a divergence of about 23 degrees at the wafer. It was necessary to provide nearly full space charge compensation to the  $^{11}B$  beam due to severe blowup over its 0.5 m path length when lower compensation values were used.

When the model of Figure 3 was run for  $B_{18}H_x^+$  with 98% space charge compensation, the angular divergence was 0.47 degrees, in good agreement with the measured data of Figure 2, suggesting that 98% compensation is a realistic value for this 2D model.



**FIGURE 3.** 10 keV, 0.42 mA  $B_{18}H_x^+$  beam terminating at the wafer, assuming 43% space charge compensation. Half the beam is shown about the positive Z-axis. The drift length is 0.5 m.

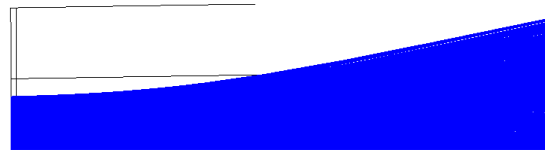


**FIGURE 4.** 500eV, 7.5 mA boron beam terminating at the wafer, assuming 98% space charge compensation. Half the beam is shown about the positive Z-axis. The drift length is 0.5 m.

Wafer charging can also affect incident beam angles. We added to the models used to generate Figure 3 and Figure 4 a photoresist-covered surface charged to 50V, which showed that the  $^{11}B^+$  beam and  $B_{18}H_x^+$  beams respond differently to the surface fields. Due to the higher stiffness and reduced charge density of the molecular beam, there is a negligible increase in divergence, while the lighter boron beam is deflected by the charged surface to a greater degree, increasing divergence by 9% from 22.9 degrees to 25 degrees.

Estimates of the plasma density needed for a complete suppression of low energy beam self-repulsion for  $B^+$  beams, so that the plasma Debye length is less than the ion spacing, leads to densities of  $>10^{12}$  ions/cm<sup>3</sup> for 1 keV  $B^+$  beams with modest electron temperatures,  $>3$  eV [11]. These plasmas would be 2 orders of magnitude denser than typical support plasmas used to suppress charging effects on device wafer surfaces.

Given the angular divergence results, we can deduce that the beam transmission through a patterned feature, for example through a via for the S/D contact plug (which can include aspect ratios as high as 100:1), will be significantly reduced for large-divergence beams. These implants tend to be low energy and high dose, e.g., as low as 1 keV at  $>1E16$  dose for 32 nm devices. A much higher total dose would be required for large-divergence beams relative to well-collimated beams, reducing wafer throughput.

## SUMMARY

Beam current and full divergence angle has been measured over the effective energy range 200eV—3keV using  $B_{18}H_{22}$  feed material in a hybrid magnetically scanned beam line. The full beam divergence was kept below about 0.5 deg over the energy range, resulting in reduced beam current at low energies. Fitting of the data showed that below about 1 keV boron energy (20 keV  $B_{18}H_x^+$  energy), the beam current was proportional to  $V^{1.5}$ , indicating that beam transmission was limited by space charge. Above 1 keV, beam current was found to be proportional to  $V^{0.45}$ , indicating that beam transmission was limited by matching of the beam emittance to the acceptance of the beam line. Transport models were constructed of two ion beams, the first carrying 7.5 mA of  $^{11}B^+$  at 500 eV, the second carrying 0.42 mA of  $B_{18}H_x^+$  beam at 10 keV. The degree of space charge compensation was varied from about 43% to 98%. The 98% case yielded significant differences between the monomer and cluster beams, the full divergence angles at the wafer being about 23 degrees for the former, and about 0.5 degrees for the latter. The model was extended to include a charged wafer surface, which resulted in a 9% increase in the divergence of the monomer beam, and a negligible increase in divergence of the cluster beam.

## REFERENCES

1. H-J. Gossmann, G. Redindo, Y. Eurokin, T. Romig, K. Elshot, J-J. Xu, J. McComb, *Solid State Technology*, July 2007, 71-76.
2. M.I. Current, D. Lopes, M.A. Foad, J.G. England, C. Jones, D. Su, *J. Vac. Sci. Technol.* **B16**(1) (1998) 327-333.
3. W. Lucaszek, M.I. Current, S. Daryanani, L. Larson, T. Rhoad, J. Shields, M. Vella, D. Wagner, Proc. of Plasma and Process-Induced Damage, P2ID03, (2003).
4. K. Yako *et al.*, 68th JSAP, Hokkaido, JP, 2007.
5. K. Uejima *et al.*, Proc. IEDM07, 2007, 151-154.
6. J. Borland *et al.*, Proc. IWJT, May, 2006
7. T. Aoyama, M. Fukuda, Y. Nara, S. Umisedo, N. Hamamoto, M. Tanjo, T. Nagayama, Internat. Workshop on Junction Technol., IWJT-05 (2005).
8. H. Glavish *et al.*, Proc. IIT2006, Marseilles, France (2006) pp. 167-170.
9. Nariaki Hamamoto *et al.*, 7th Int. Workshop on Junction Technol., June 8—9, 2007, Kyoto, Japan.
10. Lorentz User's Guide Ch. 4, Integrated Engineering Software, Inc.
11. M.I. Current, W. Lucaszek, M.C Vella, Proc. of 5th Inter. Symp. on Plasma Process-induced Damage, P2ID-2000, pp 137-140 (2000).
12. K. Okabe *et al.*, these proceedings, and references contained therein; also Fujitsu, IWJT 2005.